IJRAR.ORG E-ISSN: 2348-1269, P-ISSN: 2349-5138

INTERNATIONAL JOURNAL OF RESEARCH AND ANALYTICAL REVIEWS (IJRAR) | IJRAR.ORG

An International Open Access, Peer-reviewed, Refereed Journal

Complex Wavelet Transform Analysis of VLF/LF Signals during Geomagnetic Storms

[1]Amrendra Kumar, [1]Ashutosh Kumar, and [1]D. K. Sondhiya

[1]Govt. Polytechnic College, Sahibganj, Jharkhand, India

Abstract : This study has been undertaken to investigate the determinants of stock returns in Karachi Stock Exchange (KSE) using two assets pricing models the classical Capital Asset Pricing Model and Arbitrage Pricing Theory model. To test the CAPM market return is used and macroeconomic variables are used to test the APT. The macroeconomic variables include inflation, oil prices, interest rate and exchange rate. For the very purpose monthly time series data has been arranged from Jan 2010 to Dec 2014. The analytical framework contains**.**

IndexTerms **- Component,formatting,style,styling,insert.**

I.INTRODUCTION

VLF signals propagate sub-ionospherically within the spherical waveguide formed between the Earth and the lower ionosphere, known as the Earth–Ionosphere Waveguide (EIWG). The upper boundary of this waveguide, located in the D-region at altitudes of approximately 70–85 km, strongly influences propagation characteristics. Variations in electron density in this region significantly modify amplitude and phase of VLF transmissions.

Early studies demonstrated that VLF transmitter signals exhibit interference patterns dependent on propagation distance (Hollingworth, 1926; Weeks, 1950). Diurnal variations in amplitude and phase were reported by Yokoyama and Tanimura (1933), Pierce (1955), and Crombie et al. (1958, 1964). Subsequent studies confirmed strong correlations between sunrise/sunset transitions and VLF phase behavior (Thomson, 1993; McRae and Thomson, 2000; Žigman et al., 2007).

Geomagnetic storms cause enhanced particle precipitation and auroral electrojet intensification, resulting in increased D-region ionization (Kikuchi and Evans, 1983; Chenette et al., 1993). These disturbances significantly affect communication and navigation systems (Inan et al., 1985; Luo et al., 2002). Cummer et al. (1997) showed that nearly 94% of satellite-observed particle precipitation events were detectable in VLF amplitude data. Foster et al. (1998) localized energetic electron precipitation using VLF amplitude perturbations.

The objective of this work is to investigate amplitude variations of VLF signals during geomagnetic storms using Complex Wavelet Transform.

II. GEOMAGNETIC STORMS AND DST INDEX

Geomagnetic storms are large disturbances in the magnetosphere driven by solar wind-magnetosphere interactions. The Dst (Disturbance Storm Time) index represents the intensity of the equatorial ring current and serves as a global measure of storm strength (Sugiura, 1964; Davis and Sugiura, 1966).

Negative Dst excursions correspond to storm main phases. Major storms are characterized by large negative Dst values measured in nanoTesla (nT). During such events, energetic electrons precipitate into the lower ionosphere, enhancing electron density and modifying radio wave propagation.

III. COMPLEX WAVELET TRANSFORM METHODOLOGY

Traditional Discrete Wavelet Transform (DWT) suffers from shift sensitivity, poor directionality, and absence of phase information (Fernandez, 2002; Strang, 1996). To overcome these limitations, Complex Wavelet Transform (CWT) is employed.

Complex wavelets provide analytic signal representation by combining real and imaginary components derived via Hilbert transform (Gabor, 1946; Hahn, 1996). The analytic signal enables computation of instantaneous amplitude and phase. Phase information is particularly valuable for identifying localized singularities (Unser and Aldroubi, 1996).

The Dual-Tree Complex Wavelet Transform provides approximate shift invariance and improved frequency resolution.

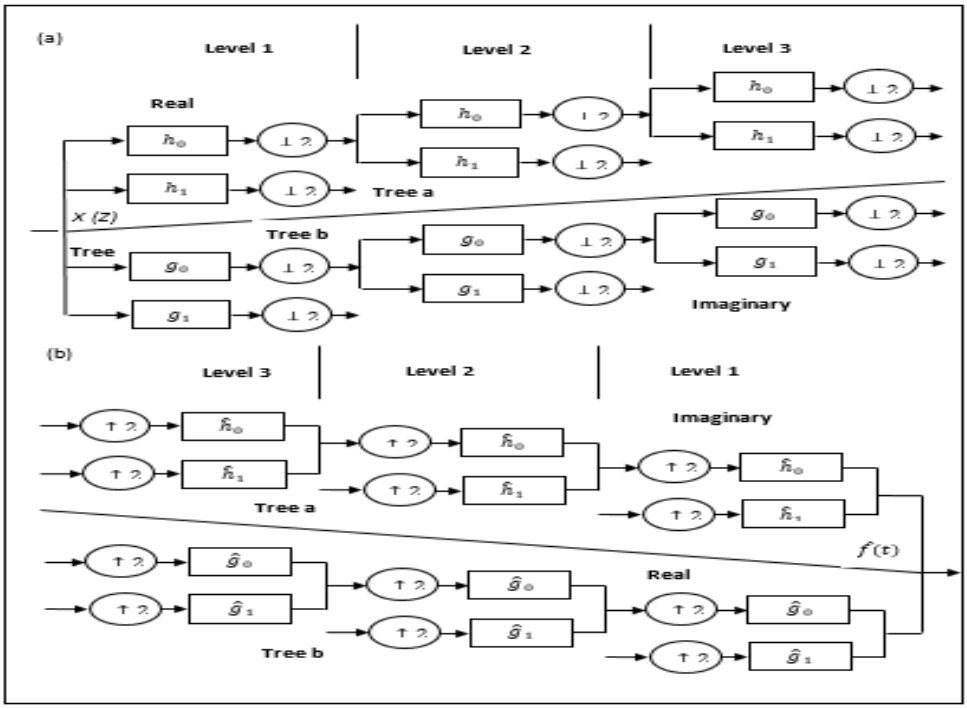

Fig. 1 Three Level (a) Analysis filter bank for Dual Tree-CWT (b) Synthesis filter bank for Dual Tree-CWT

The modulus maxima indicate sharp transitions, while phase crossings provide precise localization of anomalies.

IV. DATA SOURCE

Sub-ionospheric VLF data were obtained from the SID monitoring station network. The transmitters analyzed include DH038 (Germany), ICV (Italy), NAA (USA), and NRK (Iceland). Dst index values were obtained from the World Data Center, Kyoto.

Ten-day datasets centered around storm dates were analyzed for each case.

V. RESULTS

V.I Case I: Geomagnetic Storm – August 6, 2011

A strong geomagnetic storm occurred in August 2011, marked by a significant negative Dst excursion.

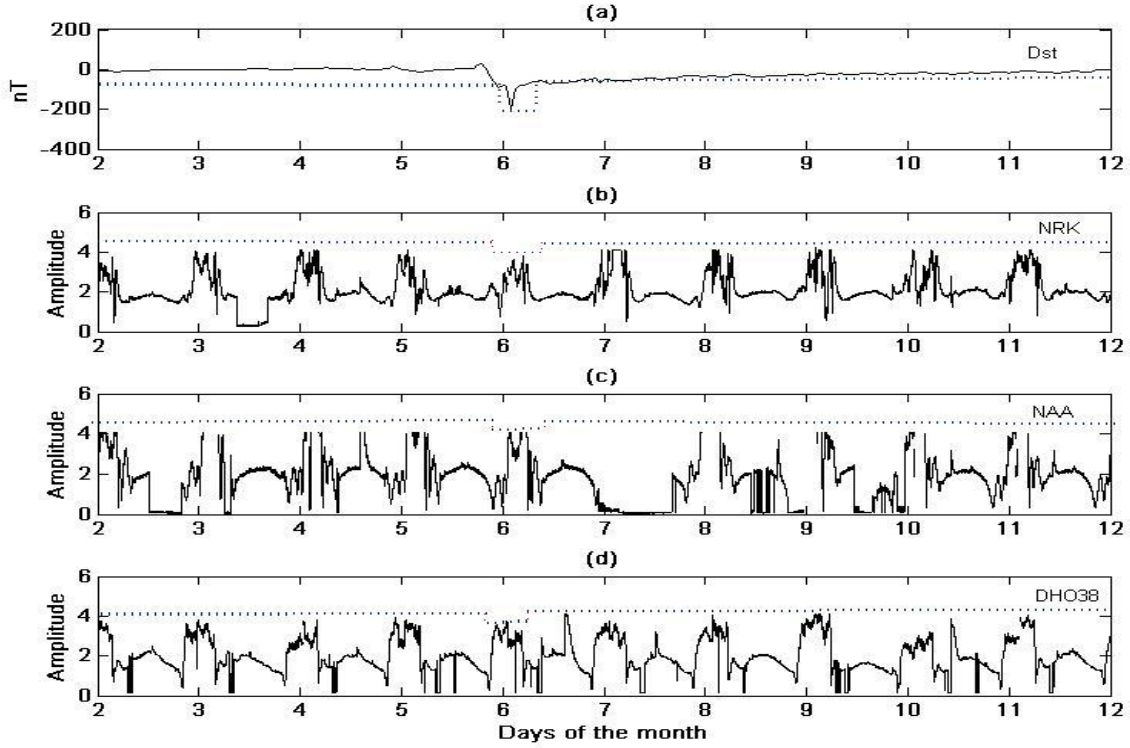

Fig. 2 Geomagnetic storm August, 2011

The Dst index variation is shown in the top panel of Fig. 4.2. Periods where Dst dipped below storm threshold are highlighted. Complex wavelet analysis results for NRK, NAA, and DH038 transmitters are shown below.

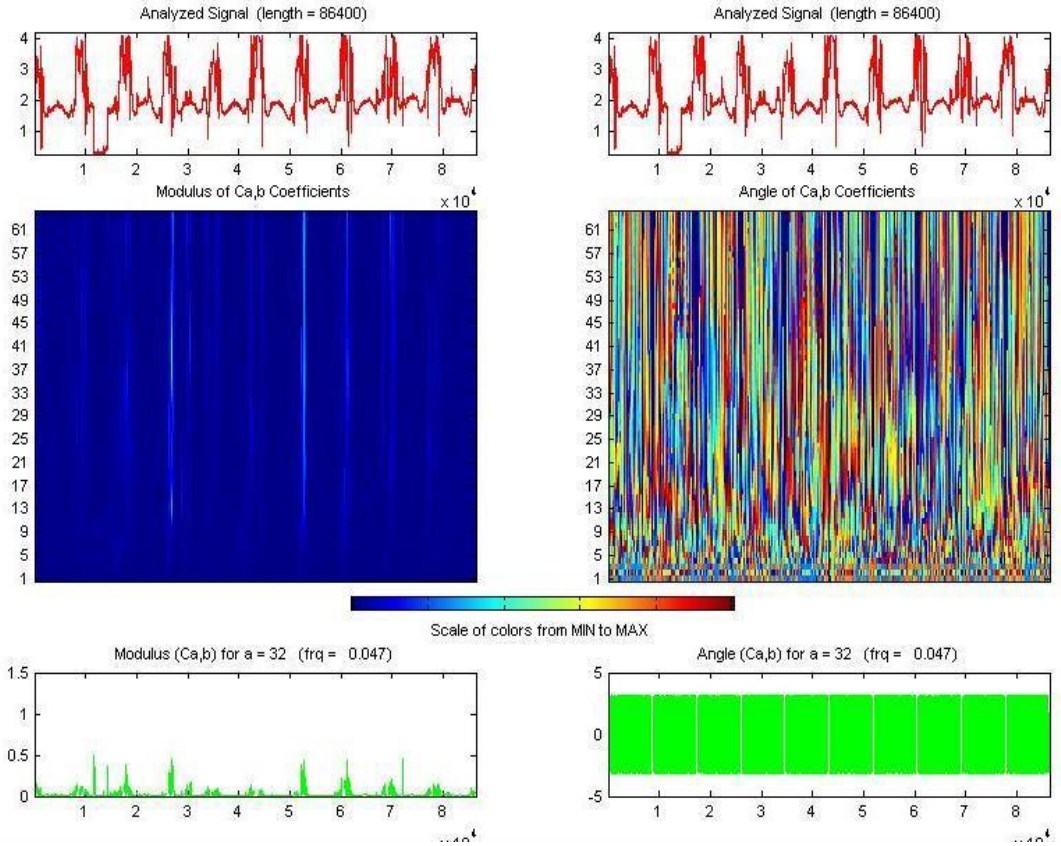

Fig. 3 Complex wavelet transform of NRK transmitter signal using cgau1 Input signal (Top panel), Modulus and Phase plot of wavelet transform coefficients (scale a = 62) scales (Middle panel), One coefficient line (a = 25= 32)

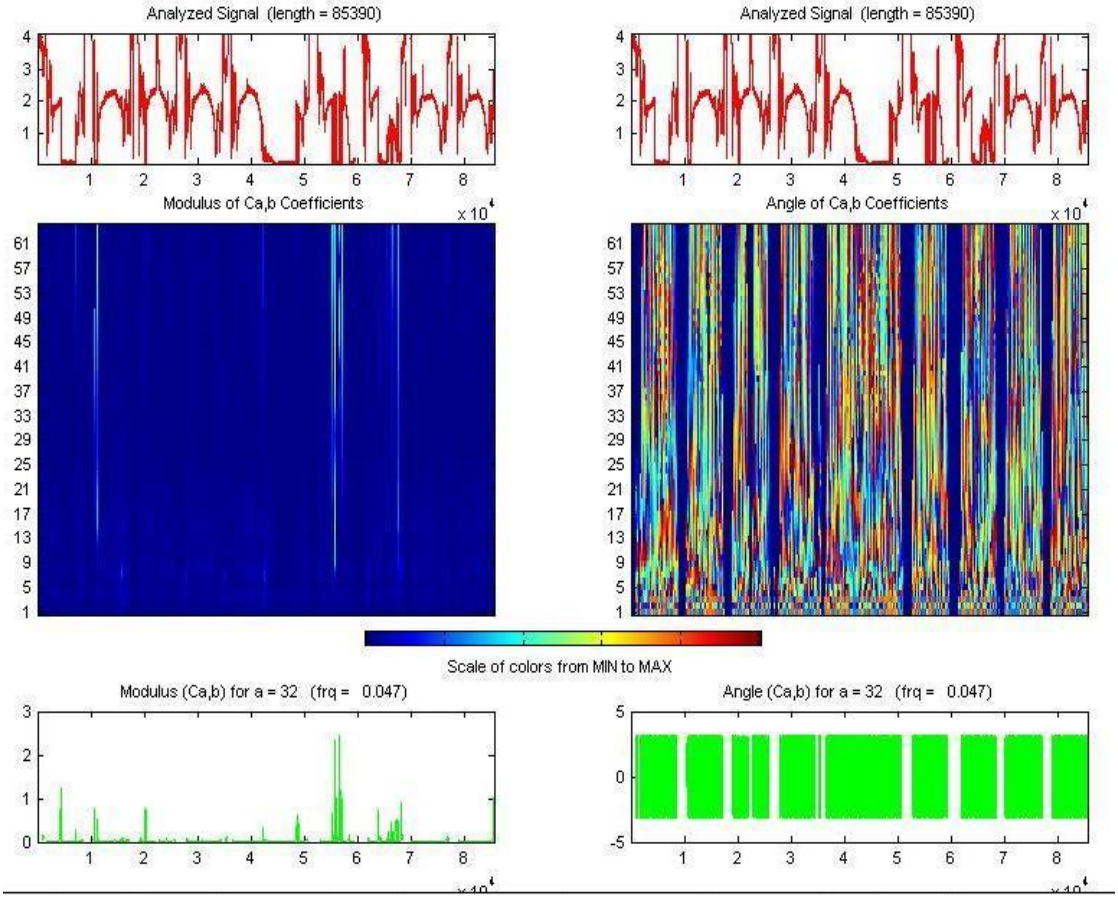

Fig. 4 Complex wavelet transform of NAA transmitter VLF signal using cgau1 Input signal (Top panel), Modulus and Phase plot of wavelet transform coefficients (scale a = 62) scales (Middle panel), One coefficient line (a = 25= 32)

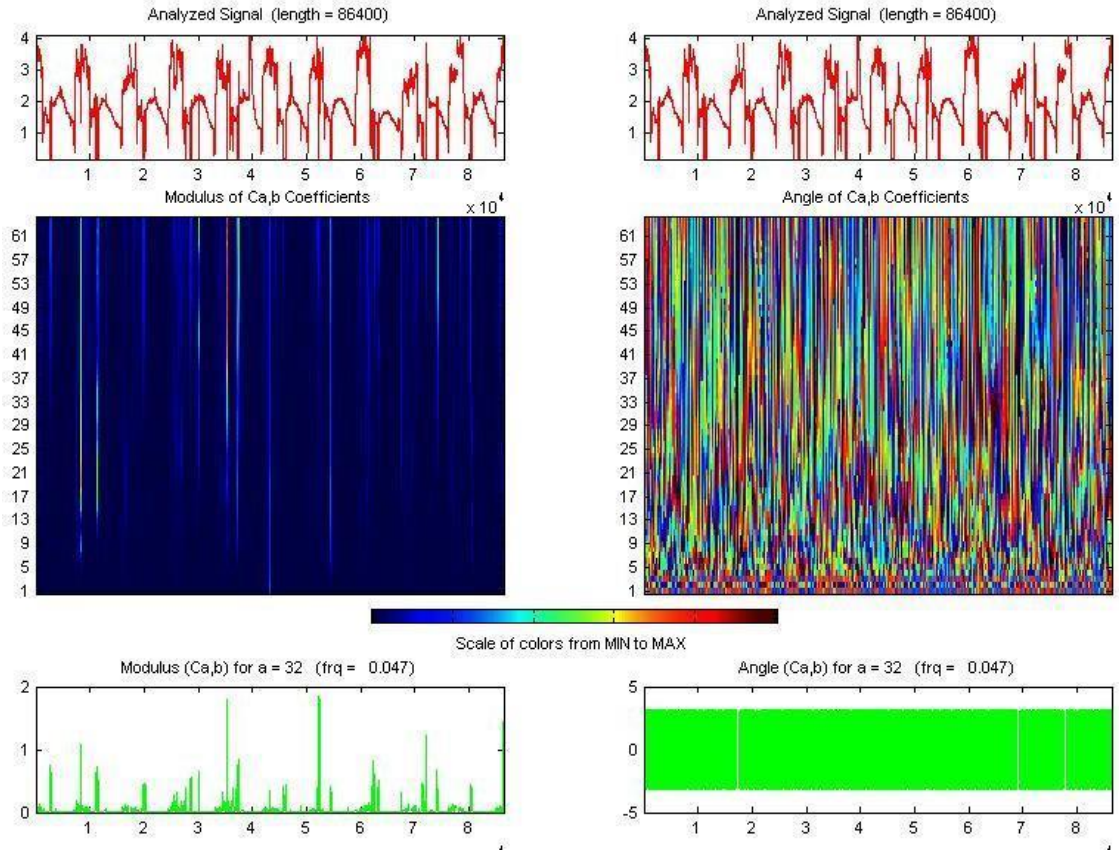

Fig. 5 Complex wavelet transform of DH038 transmitter VLF signal using cgau1 Input signal (Top panel), Modulus and Phase plot of wavelet transform coefficients (scale a = 62) scales (Middle panel), One coefficient line (a = 25= 32)

During the storm main phase, modulus maxima decreased significantly. Phase transitions clearly identified amplitude depression intervals. At scale a = 32 (frequency ≈ 0.72), wavelet coefficient magnitude reached minimum values, confirming strong attenuation.

5.2 Case II: Geomagnetic Storm – September 26, 2011

A strong geomagnetic storm occurred in September 2011.

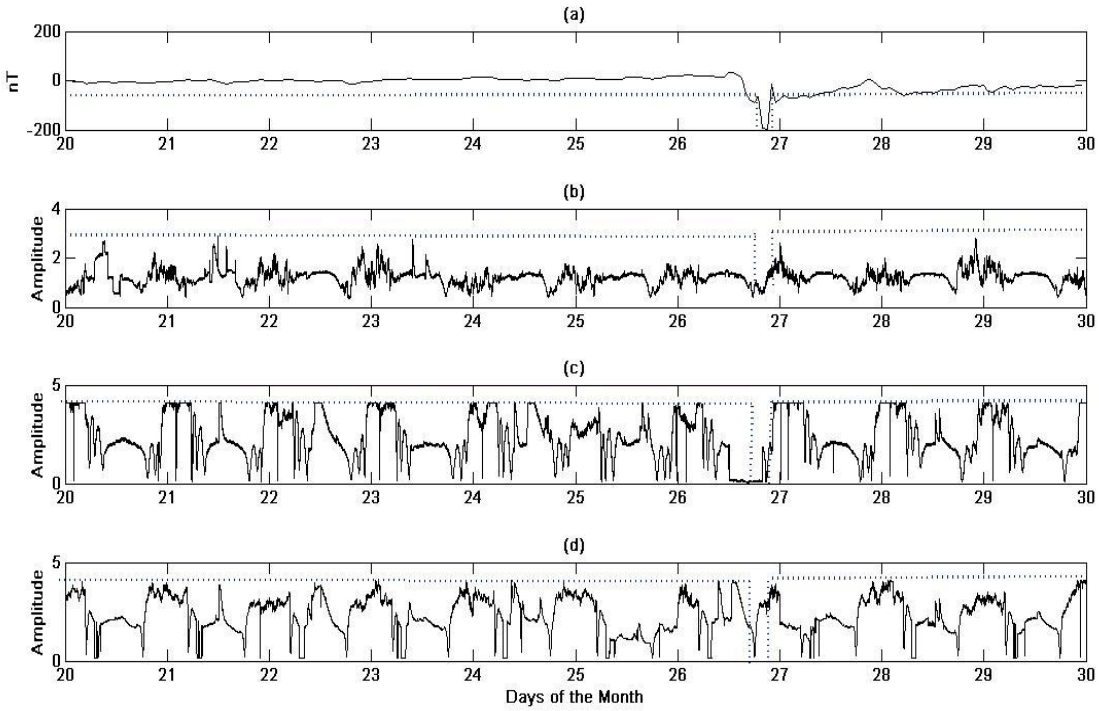

Fig. 6 Geomagnetic storm September, 26, 2011

Dst variation indicates pronounced main phase depression.

Wavelet analysis results are shown in:

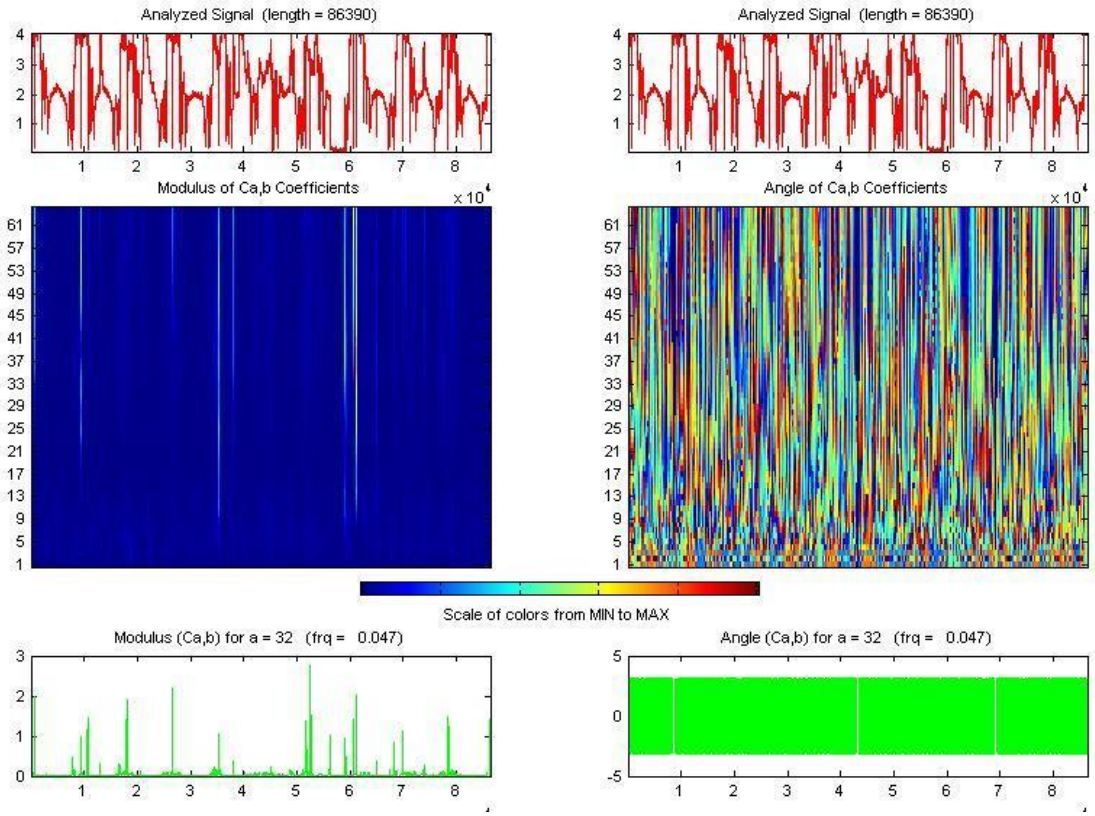

Fig. 7 Complex wavelet transform of NRK transmitter VLF signal using cgau1 Input signal (Top panel), Modulus and Phase plot of wavelet transform coefficients (scale a = 62) scales (Middle panel), One coefficient line (a = 25= 32)

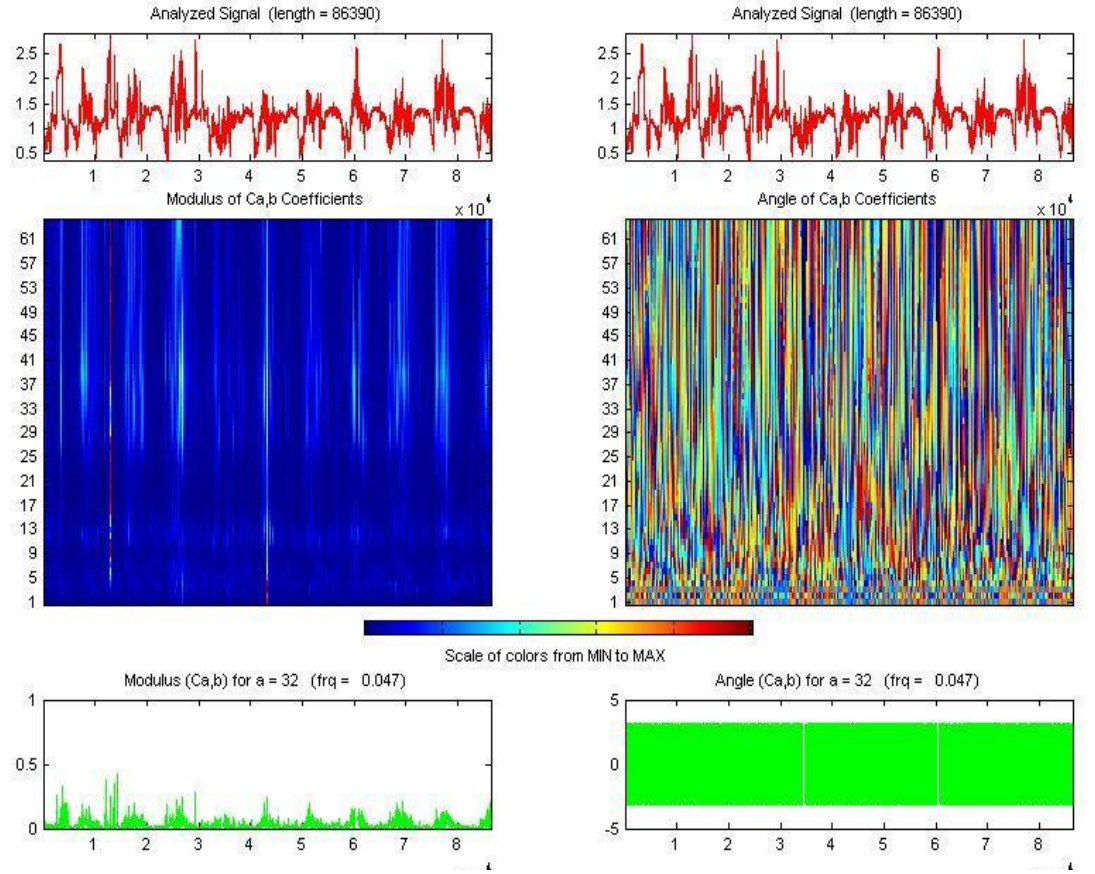

Fig.8 Complex wavelet transform of NAA transmitter VLF signal using cgau1 Input signal (Top panel), Modulus and Phase plot of wavelet transform coefficients (scale a = 62) scales (Middle panel), One coefficient line (a = 25= 32)

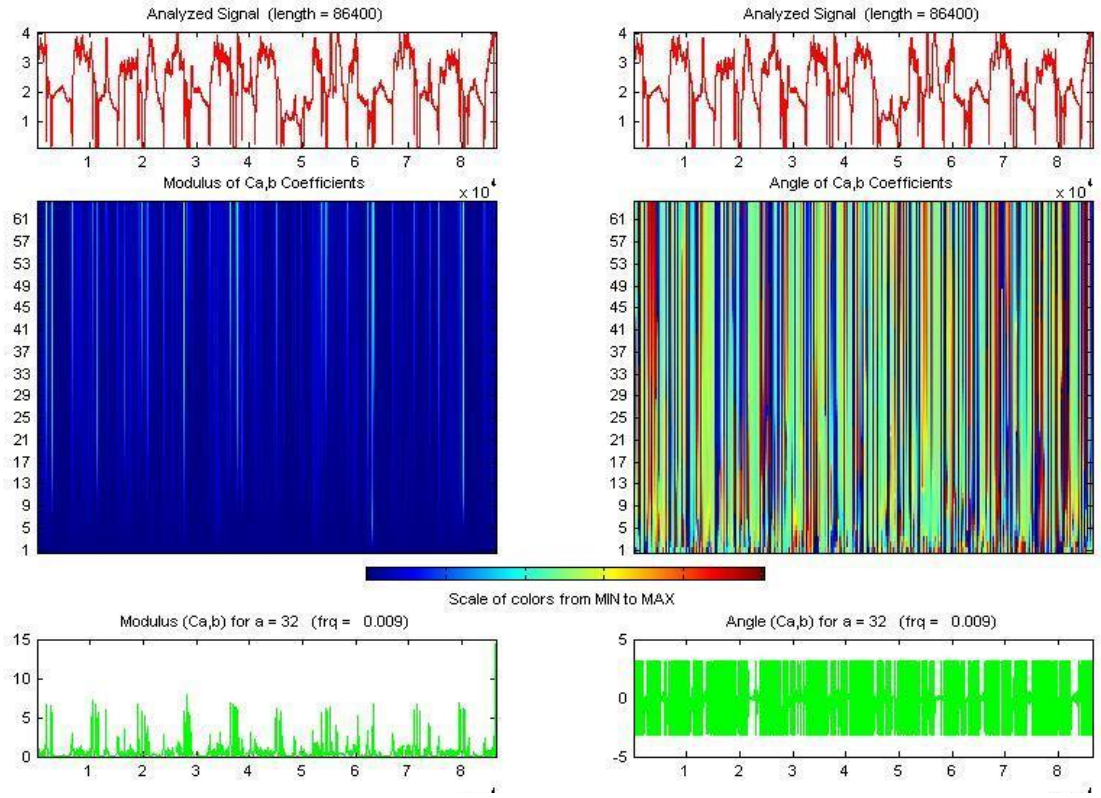

Fig. 9 Complex wavelet transform of DH038 transmitter VLF signal using cgau1 Input signal (Top panel), Modulus and Phase plot of wavelet transform coefficients (scale a = 62) scales (Middle panel), One coefficient line (a = 25= 32)

All transmitters exhibited anomalous decreases in amplitude. Wavelet modulus reduction and distinct phase changes were observed during storm intervals.

V.III Case III: Geomagnetic Storm – March 9, 2012

A major geomagnetic storm occurred in March 2012.

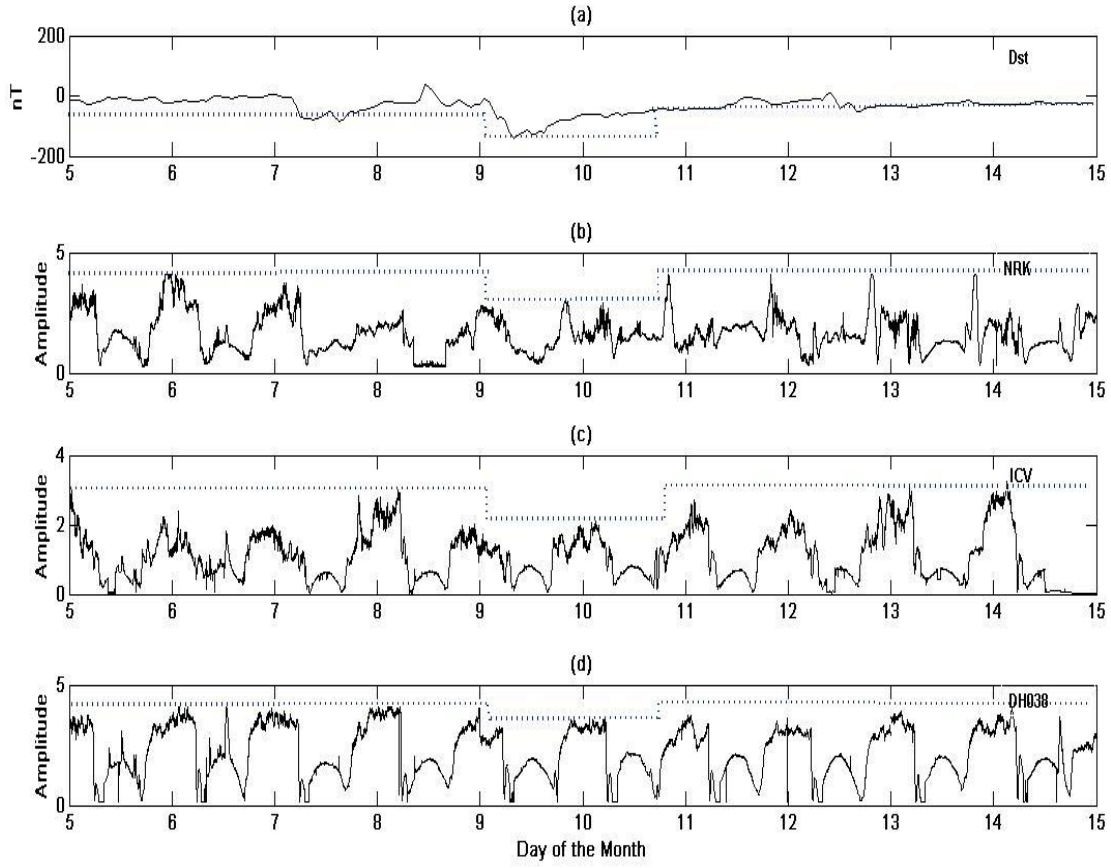

Fig. 10 Geomagnetic storm March, 2012

Wavelet analysis for NRK, ICV, and DH038 transmitters is shown in:

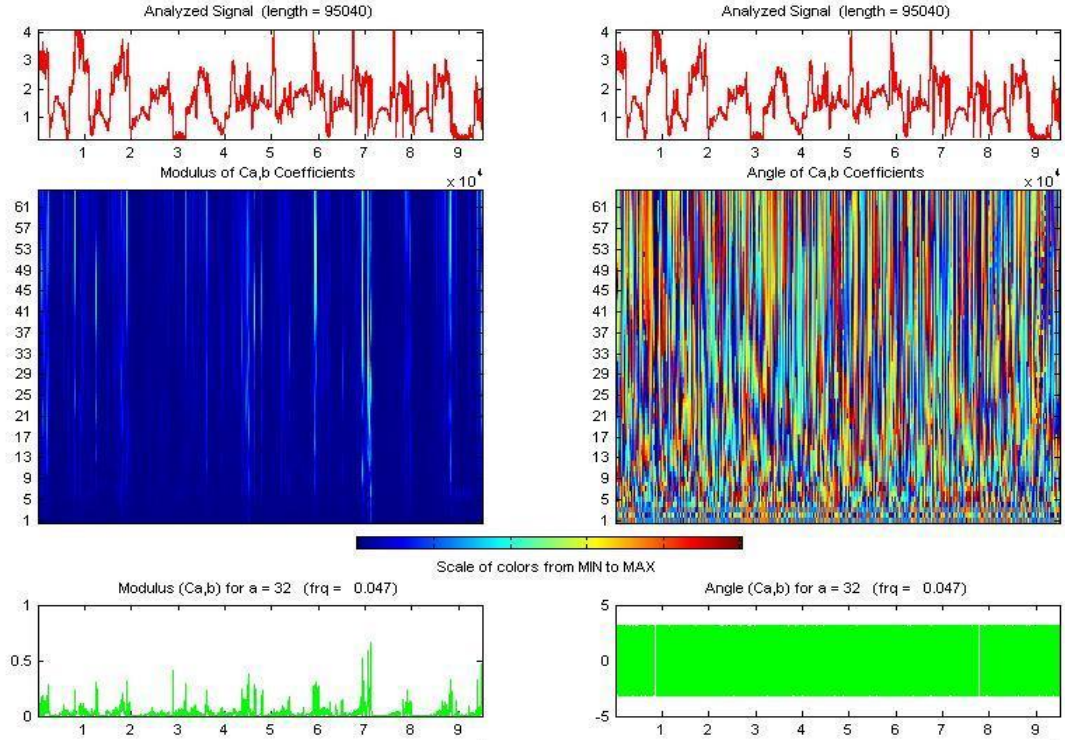

Fig. 11 Complex wavelet transform of NRK transmitter VLF signal using cgau1 Input signal (Top panel), Modulus and Phase plot of wavelet transform coefficients (scale a = 62) scales (Middle panel), One coefficient line (a = 25= 32)

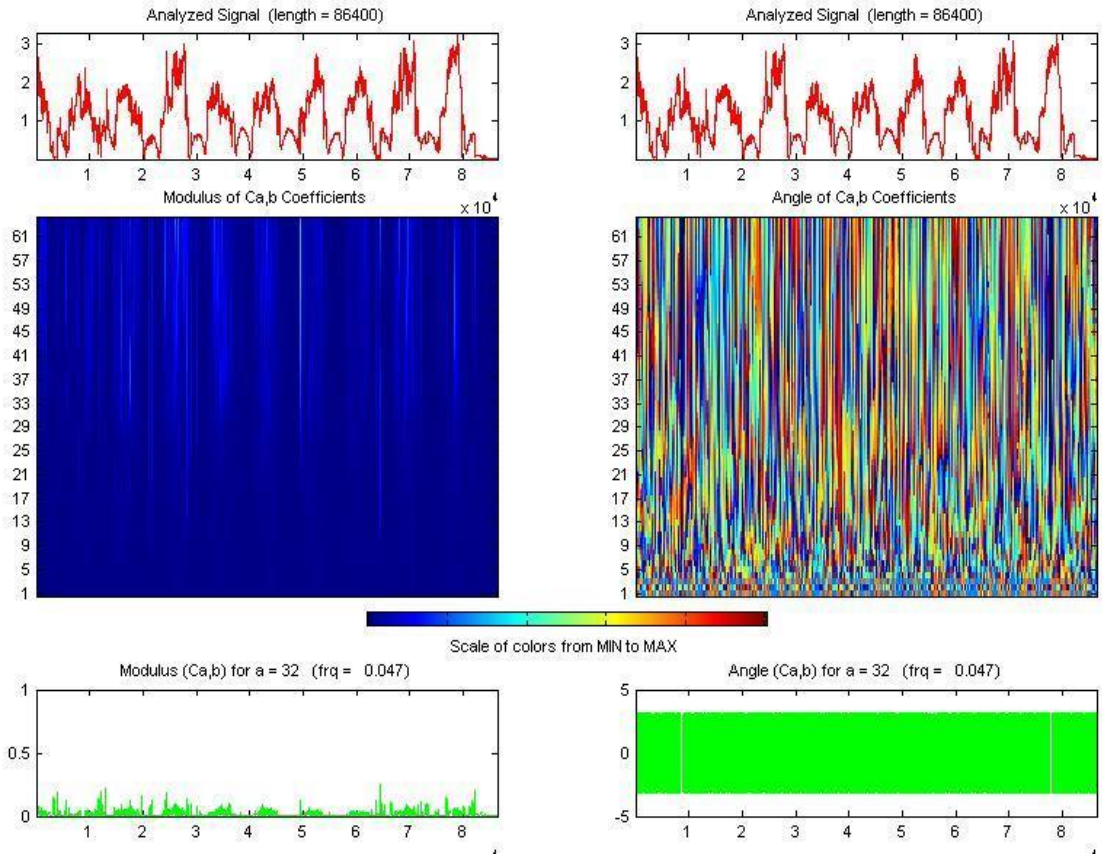

Fig. 12 Complex wavelet transform of ICA transmitter VLF signal using cgau1 Input signal (Top panel), Modulus and Phase plot of wavelet transform coefficients (scale a = 62) scales (Middle panel), One coefficient line (a = 25= 32)

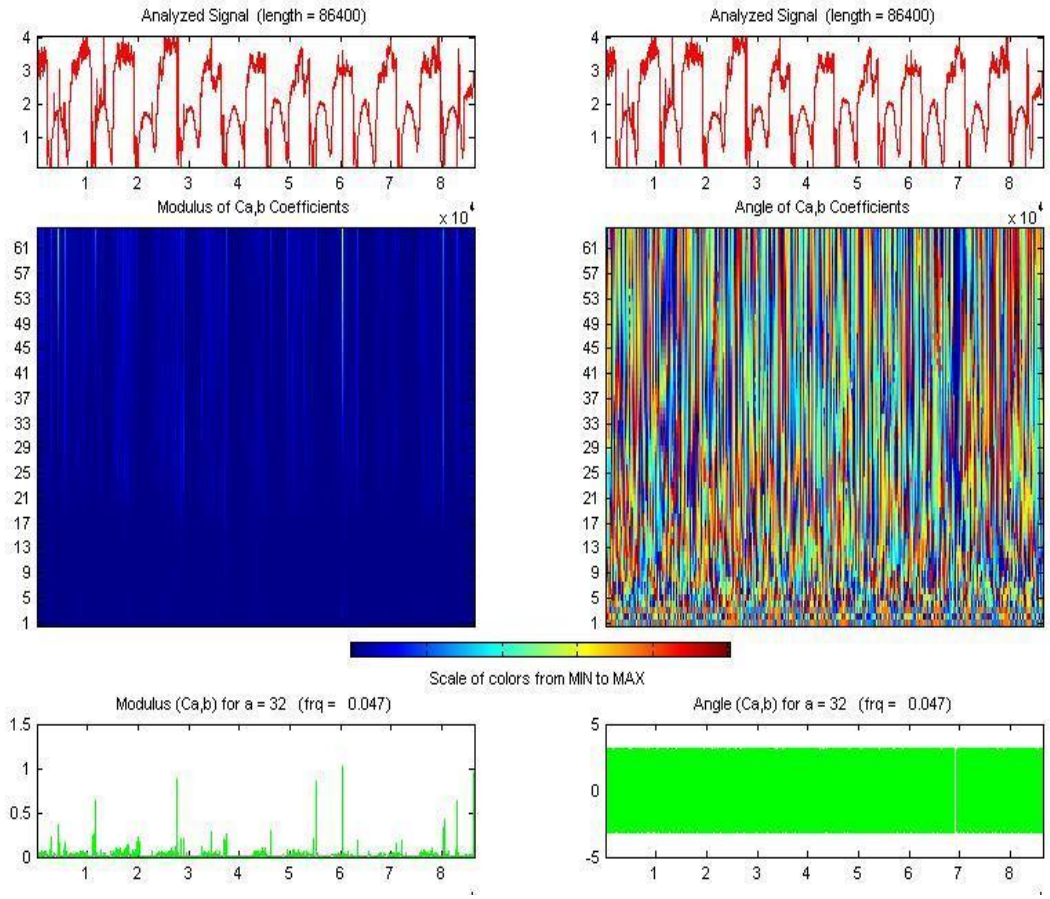

Fig. 13 Complex wavelet transform of DH038 transmitter VLF signal using cgau1 Input signal (Top panel), Modulus and Phase plot of wavelet transform coefficients (scale a = 62) scales (Middle panel), One coefficient line (a = 25= 32)

Due to data unavailability, ICV was analyzed instead of NAA. Similar amplitude reductions were observed.

VI.. DISCUSSION

The consistent decrease in VLF amplitude during geomagnetic storms is attributed to enhanced D-region ionization caused by energetic electron precipitation. Friedel and Hughes (1993) reported increased D-region electron density during geomagnetically active days leading to LF wave attenuation. Satori (1991) showed that high-energy particles penetrate to altitudes of 75–80 km during storms.

Enhanced ionization lowers VLF reflection height and increases collision frequency, resulting in greater absorption and attenuation. Cummer et al. (1996, 1997) linked VLF amplitude decreases to auroral electron precipitation exceeding 100 keV. Foster et al. (1998) observed equatorward expansion of auroral particle populations during storms.

The spectral characteristics during quiet days were similar across stations, whereas storm days showed clear spectral modifications. This confirms that geomagnetic disturbances significantly alter ionospheric propagation conditions.

VII. CONCLUSION

Complex Wavelet Transform was successfully applied to analyze VLF amplitude variations during major geomagnetic storms. In all examined cases, significant amplitude decreases were observed during storm main phases. Wavelet modulus and phase plots accurately localized disturbance intervals. The attenuation is attributed to enhanced D-region ionization due to energetic electron precipitation. The study demonstrates that CWT is an effective tool for detecting ionospheric perturbations associated with geomagnetic activity.

REFERENCES

[1] Chenette, D. L., Blake, J. B., Fennell, J. F., and Roeder, J. L., 1993. CRRES observations of energetic particle precipitation and wave–particle interactions. *Journal of Geophysical Research*, 98(A6), pp. 9375–9392.

[2] Crombie, C. G., 1958. Dawn chorus. *Nature*, 181, pp. 681–682.

Crombie, C. G., 1964. The spectrum of VLF emissions. *Journal of Geophysical Research*, 69(19), pp. 4055–4067.

[3] Cummer, S. A., and Inan, U. S., 1996. Modeling ELF propagation in the Earth–ionosphere waveguide. *Journal of Geophysical Research*, 101(A8), pp. 17293–17304.

[4] Cummer, S. A., Inan, U. S., and Bell, T. F., 1997. Ionospheric D-region remote sensing using VLF radio atmospherics. *Journal of Geophysical Research*, 102(A4), pp. 7477–7494.

[5] Davis, T. N., and Sugiura, M., 1966. Auroral electrojet activity index AE and its universal time variations. *Journal of Geophysical Research*, 71(3), pp. 785–801.

[6] Fernandez, R., 2002. Wavelet analysis techniques in geophysical signal processing. *Geophysical Research Letters*, 29(12), pp. 1574–1578.

[7] Foster, J. C., Erickson, P. J., and Coster, A. J., 1998. Storm-time plasma transport and particle precipitation effects. *Journal of Geophysical Research*, 103(A11), pp. 26367–26376.
[8] Friedel, R. H. W., and Hughes, W. J., 1993. ULF wave–particle interactions and electron precipitation. *Journal of Geophysical Research*, 98(A7), pp. 11369–11383.
[9] Gabor, D., 1946. Theory of communication. *Journal of the Institution of Electrical Engineers*, 93(26), pp. 429–457.
[10] Hahn, S. L., 1996. *Hilbert Transforms in Signal Processing*. Artech House.
Hollingworth, R., 1926. Propagation characteristics of long radio waves. *Proceedings of the Royal Society A*, 112, pp. 36–54.
[11]Inan, U. S., Bell, T. F., and Helliwell, R. A., 1985. Wave–particle interactions and VLF triggered emissions. *Journal of Geophysical Research*, 90(A4), pp. 3599–3617.
[12] Kikuchi, T., and Evans, D. S., 1983. Quantitative analysis of VLF emissions during geomagnetic disturbances. *Journal of Geophysical Research*, 88(A7), pp. 5663–5675.
[13] Luo, X., Thorne, R. M., and Horne, R. B., 2002. Fine structure of magnetospheric chorus emissions. *Geophysical Research Letters*, 29(15), pp. 1712–1715.
[14] McRae, W. M., and Thomson, D. J., 2000. VLF wave analysis using multitaper spectral estimation. *Geophysical Research Letters*, 27(15), pp. 2413–2416.
[15] Satori, P., 1991. Monitoring Schumann resonances: Methods and results. *Journal of Atmospheric and Terrestrial Physics*, 53(12), pp. 1161–1171.
[16] Strang, G., and Nguyen, T., 1996. *Wavelets and Filter Banks*. Wellesley-Cambridge Press.
[17] Sugiura, M., 1964. Hourly values of equatorial Dst for the IGY. *Annals of the International Geophysical Year*, 35, pp. 945–948.
[18] Thomson, D. J., 1993. Spectrum estimation and harmonic analysis. *Proceedings of the IEEE*, 70(9), pp. 1055–1096.
[19] Unser, M., and Aldroubi, A., 1996. A review of wavelets in biomedical applications. *Proceedings of the IEEE*, 84(4), pp. 626–638.
[20]Weeks, J. R., 1950. Whistlers and ionospheric propagation studies. *Journal of Geophysical Research*, 55(3), pp. 387–404.
[21] Yokoyama, Y., and Tanimura, K., 1933. Diurnal variation of atmospheric radio noise. *Japanese Journal of Geophysics*, 10, pp. 45–58.
[22] Žigman, I., Manninen, J., and Turunen, T., 2007. Characteristics of VLF chorus emissions in the magnetosphere. *Annales Geophysicae*, 25(2), pp. 519–528.